UBe_{13}: PROTOTYPE OF A NON-FERMI-LIQUID SUPERCONDUCTOR*

N. Oeschler, F. Kromer, T. Tayama†, K. Tenya‡, P. Gegenwart
G. Sparn, F. Steglich

Max Planck Institute for Chemical Physics of Solids
Nöthnitzer Str. 40, 01187 Dresden, Germany

M. Lang

Institute of Physics, University of Frankfurt/Main
60054 Frankfurt/Main, Germany

and G.R. Stewart

Department of Physics, University of Florida, Gainesville, FL 32611, USA

(Received July 10, 2002)

We review pronounced non-Fermi-liquid (NFL) effects in the low-temperature normal state of the heavy-fermion superconductor UBe_{13} ($T_c \approx 0.9\,K$). We argue that these NFL effects may presumably be related to short-range antiferromagnetic (AF) correlations which are manifested in the superconducting (SC) state by a "line of thermodynamic anomalies", $B^*(T)$, between $T \approx 0.7\,K$ ($B = 0$) and $B \approx 4\,T$ ($T \to 0$). These anomalies are shown to mark the precursor of the lower of the two phase transitions (at T_{c1} and T_{c2}) in $U_{1-x}Th_xBe_{13}$, $x_{c1} \approx 0.019 < x < x_{c2} \approx 0.0455$. For $x_{c2} < x < x_c < 0.07$, a single SC transition is stated which due to thermal expansion, $\alpha(T)$, and specific heat, $C(T)$, measurements, coincides with this lower transition at T_{c2}. We discuss two possible scenarios both of which imply an intimate interrelation of superconductivity with the symmetry-broken state that forms below T_{c2}. Finally, we address two other lines of thermal expansion anomalies in the T–x phase diagram of $U_{1-x}Th_xBe_{13}$ which show an only weak dependence on magnetic field: *(i)* A positive $\alpha(T)$ peak, along with a $C(T)$ peak, is found in pure UBe_{13} at $T_{max} \approx 2\,K$.

* Presented at the International Conference on Strongly Correlated Electron Systems, (SCES 02), Cracow, Poland, July 10–13, 2002.

† Present address: Institute for Solid State Physics, University of Tokyo, Kashiwa, Japan

‡ Present address: Hokkaido University, Sapporo 060-0810, Japan

Upon Th doping, $T_{\max}(x)$ is depressed linearly and vanishes close to the upper critical Th concentration x_{c2} at which the two phase transitions merge to one. *(ii)* A negative anomaly in $\alpha(T)$ develops for $x > x_{c2}$ at $T_{\min}$. $T_{\min}(x)$ increases by more than a factor of two when raising the Th content to $x = 0.1$. Similar to previous results by Aliev *et al.* [F.G. Aliev *et al.*, *J. Phys.: Condens. Matter* **8**, 9807 (1995)], an almost temperature-independent non-linear susceptibility, $\chi^{(3)}(T)$, is found for $U_{0.9}Th_{0.1}Be_{13}$, at striking variance to $\chi^{(3)}(T)$ for pure UBe_{13}. The implications of this observation for the assignment of the valence state of Uranium at $x = 0$ and $x = 0.1$ are also addressed.

PACS numbers: 74.25.Bt, 74.70.Tx

1. Introduction

Strongly correlated electron systems in a metallic environment remain one of the outstanding problems in condensed-matter physics. Certain lanthanide- and actinide-based intermetallics, the so-called heavy-fermion metals, are particularly well suited to study strongly correlated electron systems. While at high temperatures these materials contain a dense lattice of local $4f/5f$ moments only weakly coupled to the Fermi sea of itinerant (s, p, d) conduction electrons, well below some characteristic temperature T^* ($\approx$ 10–100 K), the local moments become progressively reduced, and simultaneously new quasiparticles are formed. These "heavy fermions" (HF) resemble the conduction electrons of a simple metal but acquire a huge effective mass m^*, up to a thousand times greater than the free-electron mass as estimated from the large electronic specific heat at low T. HF might be called "composite fermions" consisting of a dominating local f (the "heavy") component with some admixture of delocalized conduction-electron ("light") contributions.

Residual interactions between HF frequently appear to result in broken-symmetry states at low T. For example, a heavy Landau–Fermi-liquid (LFL) state is found to coexist with small-moment antiferromagnetic (AF) order below T_N ($\approx$ 10 K) [1]. At even lower temperatures ($T \leq 1$ K), the LFL state in these systems becomes unstable against a superconducting (SC) transition and HF superconductivity coexists with AF order below T_c (≤ 1 K) [1].

An increasing number of HF metals, however, do not achieve a LFL state but rather exhibit strong non-Fermi-liquid (NFL) properties at low temperatures [2]. In most cases NFL behaviour can be related to the vicinity of an AF quantum-critical point (QCP). Examples are $CeCu_2Si_2$ and $CeCoIn_5$, the first [3] and one of the most recently [4] discovered HF superconductors. For such systems, the possibility of a spin-fluctuation-mediated pairing mechanism is currently the subject of controversial discussion.

The cubic compound UBe_{13} is a particularly fascinating example of a "NFL superconductor" [5]. Its HF-SC state forms below $T_c \approx 0.9\,K$ out of a normal state that is dominated by strong incoherent scattering characterised by an extremely large and strongly T-dependent electrical resistivity and a rather low magnetic susceptibility [5]. This has led to the proposal [6] that *(i)* the valence state of Uranium is $4+$ ($5f^2$) with a low-lying non-magnetic Γ_3 crystal field (CF)-derived doublet state, and *(ii)* a two-channel quadrupolar Kondo effect is responsible for UBe_{13} behaving as an "incoherent metal". On the other hand, CF effects studied via specific heat [7] and Raman-scattering [8] experiments as well as measurements of the non-linear susceptibility [9] seem to support a trivalent ($5f^3$) configuration. Special interest in UBe_{13} arose because of the complex T–x phase diagram of $U_{1-x}Th_xBe_{13}$, with the occurrence of a double-phase transition for low Th concentration [10]. This will be explored in Sect. 3. following a brief discussion of the exotic normal (N)-state and SC properties of un-doped UBe_{13} (Sect. 2). The paper is concluded in Sect. 4.

2. Low-T properties of UBe_{13}

Two variants of UBe_{13} with markedly different SC and N-state properties have been recently identified [11]: While "H-type" UBe_{13} exhibits T_c values between 0.85 K and 0.9 K, "L-type" UBe_{13} is characterised by $T_c \approx 0.75\,K$. Most polycrystalline samples reported are of type H, while all L-type samples are single crystals. In the following we discuss the low-T properties of high-quality UBe_{13} single crystals of the "H-type" variant.

As shown in Fig. 1(a), the specific heat of UBe_{13} shows an anomalous enhancement in the SC state that develops below about 0.7 K. Assuming an axial symmetry of the SC order parameter [12], we can fit the specific heat data for $0.7\,K \leq T \leq T_c$ (dotted line in Fig. 1(a) [13]) and by extrapolating this to low T can obtain an estimate for the additional contribution (inset of Fig. 1). The latter would be even larger at low temperatures if one would assume an isotropic SC order parameter for which the low-T specific heat varies exponentially instead of showing a cubic T dependence. Our measurements of the linear thermal expansion coefficient $\alpha(T)$ shown in Fig. 2 provide more direct evidence for an additional anomaly below T_c. By projecting the width of the SC transition from the $C(T)$ onto the $\alpha(T)$ data (vertical dotted lines in Fig. 2) we find that upon cooling, the SC transition manifests itself in the steep decrease in $\alpha(T)$ at $T_c \simeq 0.9\,K$, thus leaving the broadened minimum as an independent anomaly [14]. This assignment is corroborated by a thermodynamic analysis of the SC transition. Employing the construction as indicated in Fig. 2 to extract the $\alpha(T)$ discontinuity at T_c, $\Delta\alpha^{sc}$, we are able to calculate the initial hydrostatic-pressure dependence of T_c

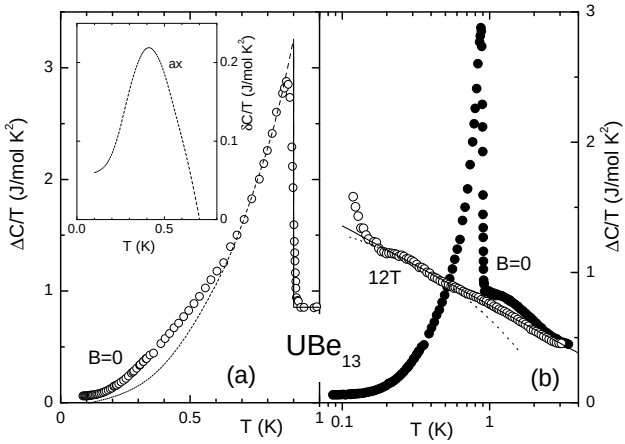

Fig. 1. Specific heat $\Delta C = C - C_{\rm nuclear}$ of a UBe_{13} single crystal as $\Delta C/T$ *vs* T on a linear scale ($B = 0$) (a) and on a logarithmic scale for the same sample at $B = 0$ and 12 T (b). Dotted line in (a) indicates the quasiparticle contribution C_{ax} assuming an axial SC order parameter [13]. Inset shows the extra contribution observed in the quasiparticle specific heat, $\delta C = \Delta C - C_{ax}$, as $\delta C/T$ *vs* T. Solid and dotted lines in (b) represent $\Delta C/T \sim \log(T_0/T)$ and $\Delta C/T = \gamma_0 - \beta\sqrt{T}$, respectively.

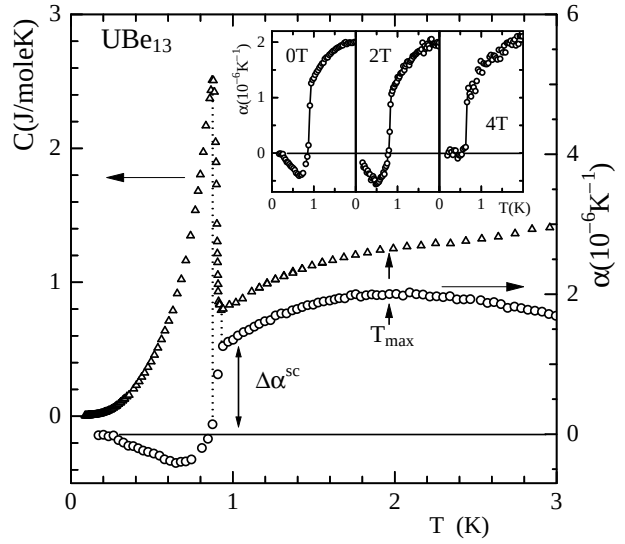

Fig. 2. Low-T specific heat and thermal expansion of a UBe_{13} single crystal. Width of SC transition is indicated by the vertical dotted lines. Vertical arrows indicate the position of the "2 K maximum" (see text). Inset shows α *vs* T at varying fields.

by means of the Ehrenfest relation, $(\partial T_c/\partial p)_{p\to 0} = V_{mol}\, T_c\, (3\,\Delta\alpha^{sc}/\Delta C^{sc})$, where $V_{mol} = 81.3\,cm^3/mol$ is the molar volume. The so-derived pressure coefficient of $(\partial T_c/\partial p)_{p\to 0} = -(13 \pm 4)\,mK/kbar$ is in excellent agreement with the results of pressure studies, $-(13 \pm 4)\,mK/kbar$ [15]. An investigation of the field dependence of $\alpha(T)$ reveals that the minimum in $\alpha(T)$ is almost completely suppressed by a field of 4 T which has, however, little effect on the SC transition (inset of Fig. 2).

As in the $\alpha(T)$ data, *cf.* inset of Fig. 2, the anomaly in specific heat measurements performed as a function of temperature at $B = 2\,T$ can be seen more clearly [13]. In Fig. 3, we display $C(B, T = \text{const.})/T$ data taken at various temperatures and indicate that, like the SC–N transition at B_{c2}, the observed features may be replaced by idealised jumps. From these isothermal field scans of the specific heat as well as from the $\alpha(T)$ measurements at constant fields shown in the inset of Fig. 2, a line of anomalies $B^*(T)$ has been established in the B–T phase diagram of UBe_{13} (Fig. 3(b)).

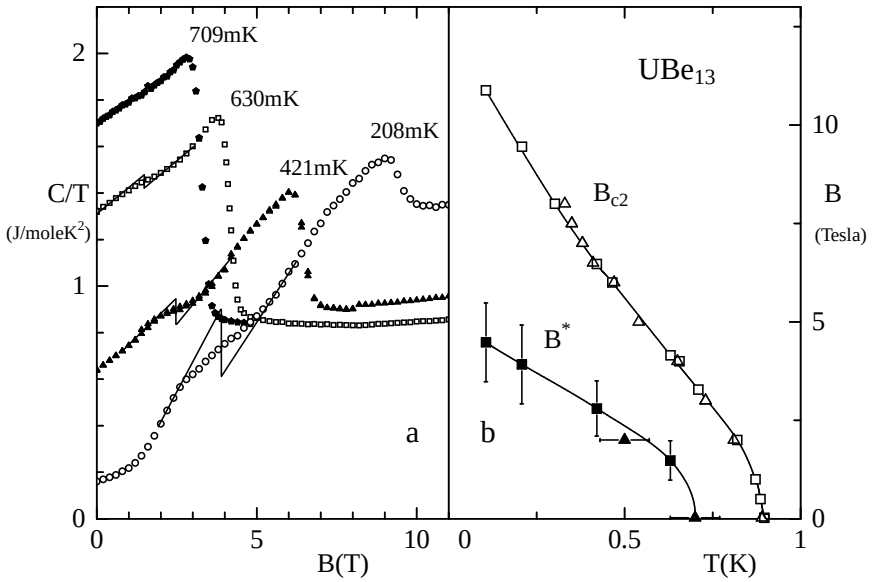

Fig. 3. (a) Low-temperature specific heat as C/T *vs* B at varying temperatures of single-crystalline UBe_{13}. (b) Corresponding B–T phase diagram including the upper critical field, $B_{c2}(T)$, as determined by specific heat (open squares) and thermal expansion (open triangles) as well as positions of anomalies observed as a function of either temperature in $\alpha(T, B = \text{const.})$ (solid triangles) or magnetic field in $C(T = \text{const.}, B)/T$ (solid squares), giving rise to a line of anomalies, $B^*(T)$.

In the following we concentrate on the N-state properties of UBe_{13}. In addition to the characteristic scale T^* whose estimates range from 8 K [7] to 30 K [16], accounting for the extremely large effective carrier masses, there exists at least one more low-energy scale in UBe_{13}. The latter manifests itself in a distinct maximum in the thermal expansion coefficient and a less pronounced shoulder in the specific heat around 2 K, see Fig. 2. Our measurements of the thermal expansion coefficient α, discussed below, show that these "2 K fluctuations" are reminiscent of local spin fluctuations in disordered Kondo systems. The "2 K fluctuations" manifest themselves also in a pronounced maximum in the resistivity around 2 K [16].

From the maximum value of $\rho(T)$, an inelastic mean free path as short as a few lattice spacings can be inferred. As demonstrated in Fig. 4(a), already moderate fields are apt to suppress this fluctuation contribution very efficiently. In a wide field range, $4\,\mathrm{T} \leq B \leq 10\,\mathrm{T}$, we are able to scale the

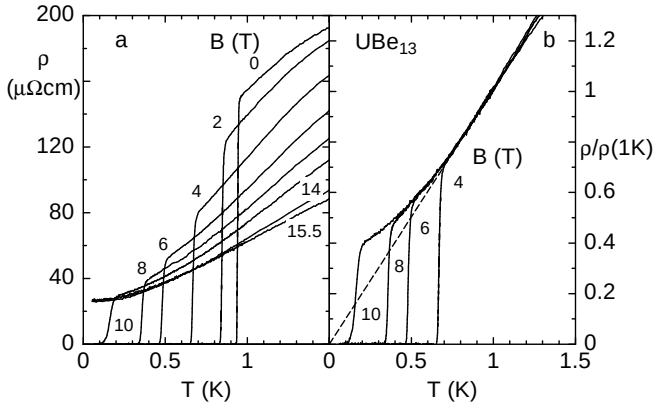

Fig. 4. (a) ρ *vs* T for a UBe_{13} single crystal at $B = 0$ and differing fields; (b) the same data as in (a), normalised to the respective $\rho(T)$ value at $T = 1\,\mathrm{K}$. Dashed line is an extrapolation to $T = 0$ of the data for $T \geq 0.8\,\mathrm{K}$.

various $\rho(T)$ curves within $T_c(B) \leq T \leq 1.2\,\mathrm{K}$ to a universal curve, by normalising $\rho(T)$ by its respective value at 1 K (Fig. 4(b)). Above $T \simeq 0.8\,\mathrm{K}$, a linear $\rho(T)$ dependence is found that can be extrapolated to $\rho = 0$ for $T \to 0$. At lower temperatures the data follow a $\rho(T) = \rho_0 + bT^{3/2}$ dependence [17]. Apparently, this T dependence is in full accord with the theoretical prediction for a three-dimensional system of itinerant AF spin fluctuations in the vicinity of a QCP [18]. As shown in Fig. 1(b), the specific heat coefficient follows $C/T \sim -\log T$ for $T > 0.3\,\mathrm{K}$ and gradually deviates to smaller values at lower T before a upturn sets in at lowest T. In the limited T range

$0.15\,\mathrm{K} \leq T \leq 0.4\,\mathrm{K}$, the specific heat coefficient can be satisfactorily described by the dependence $\Delta C/T = \gamma_0 - \beta\sqrt{T}$ that would correspond to the $T^{3/2}$ behaviour observed in $\Delta\rho(T) = \rho(T) - \rho_0$ [18]. A more detailed analysis of the $\Delta C(T)/T$ results is prevented by the up-turn below 0.2 K whose origin is not yet resolved, as the nuclear contribution due to the Zeeman splitting of the ^{9}Be spin states has already been subtracted from the raw data. For fields larger than 14 T, the low-T resistivity turns to a $\Delta\rho \sim T^2$ behaviour below 0.3 K, indicative of a magnetic field-induced Landau–Fermi-liquid state with a gigantic coefficient A. The latter is decreasing with increasing B from 52 $\mu\Omega$cm at 14 T to 45 $\mu\Omega$cm at 15.5 T [17].

To summarize, the NFL properties found for UBe_{13} are consistent with the nearness of an AF QCP at magnetic fields of about 4 T. Remarkably, this field coincides with the line of anomalies, $B^*(T)$, for $T \to 0$ which has been established in the B–T phase diagram of Fig. 3(b). Thus, one would speculate that the pronounced NFL effects observed in the N-state properties are related to the QCP ($T_\mathrm{L} \to 0$ at about 4 T). A more detailed analysis of the low-T N-state properties of UBe_{13} is, however, hampered by the large value of the upper critical field necessary to suppress superconductivity.

3. T–x phase diagram of $U_{1-x}Th_xBe_{13}$

By substituting a small amount of Th for U in UBe_{13} one observes unusual phenomena, such as a non-monotonic evolution of T_c and the occurrence of a second phase transition in a critical concentration range $x_{\mathrm{c}1} = 0.019 < x < x_{\mathrm{c}2} = 0.0455$. The most recent version of the phase diagram of $U_{1-x}Th_xBe_{13}$ [19] is shown in Fig. 5. Superconductivity occurs in pure UBe_{13} at $T_\mathrm{c} \simeq 0.9\,\mathrm{K}$, followed by the second anomaly at $T_\mathrm{L} < T_\mathrm{c}$ as discussed in the previous section. For $x < x_{\mathrm{c}1}$ doping with Th leads to a linear decrease of T_c upon increasing x. Between $x_{\mathrm{c}1}$ and $x_{\mathrm{c}2}$ two phase transitions show up. The first one at $T_{\mathrm{c}1}$ marks the appearance of superconductivity, while the nature of the second is not yet resolved. The existence of very small magnetic moments of $\mu_\mathrm{s} = 10^{-3}\,\mu_\mathrm{B}$/U below $T_{\mathrm{c}2}$ has been deduced by looking at muon-spin-relaxation (μSR) studies [21]. Ultrasound-attenuation measurements reveal indications for an AF, *i.e.* a spin-density-wave, transition which coexists with superconductivity [22]. On the other hand, a SC nature of the transition below $T_{\mathrm{c}2}$ has been claimed on the basis of lower-critical-field results [23].

Theoretical models have been proposed based on the assumption of SC states with different anisotropies for the different regions of the phase diagram [24]. The onset of small magnetic moments below $T_{\mathrm{c}2}$ is explained either by assuming an AF transition coexisting with superconductivity [24] or by broken time-reversal symmetry [25]. In these models it is assumed that

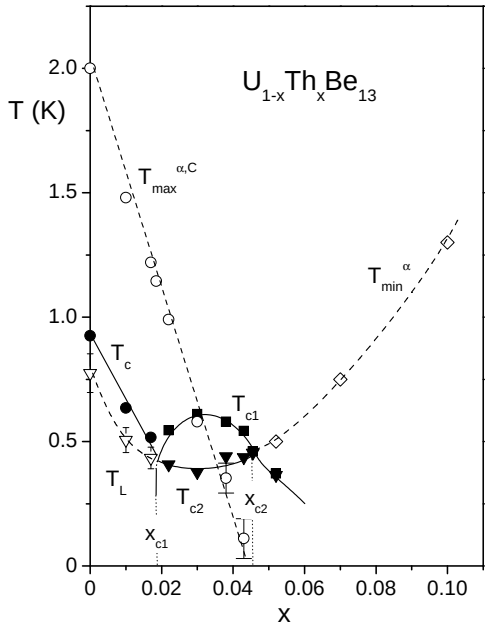

Fig. 5. T–x phase diagram of $U_{1-x}Th_xBe_{13}$. Filled symbols ascribe phase transitions, open symbols indicate anomalies. The solid vertical line at $x = x_{c1}$ reflects a phase boundary established via specific heat experiments under pressure by Zieve *et al.* [20].

$T_{c2}(x)$ is the continuation of $T_c(x)$, $x < x_{c1}$, and that this line is crossing, at $x = x_{c1}$, another phase boundary which is identical with $T_{c1}(x)$ for $x > x_{c1}$. In fact, a x-independent low-T phase boundary has been established through specific heat experiments under pressure between 0.3 K and 0.38 K and has been assigned to the second of these two crossing phase boundaries [20].

By further doping with Th, T_{c1} and T_{c2} merge at the second critical concentration x_{c2}, such that for $x > x_{c2}$ only one transition is observed. The position of the "2 K maximum" anomaly, T_{max}, observed in the N-state of UBe_{13} decreases linearly with increasing x and crosses the $T_{c1}(x)$ curve at $x \simeq 0.03$. Suppressing superconductivity by overcritical fields allows one to determine the linear dependence of $T_{max}(x)$ to higher Th concentrations.

The N-state in the region with $x > x_{c2}$ is dominated by a low-T minimum structure in the thermal expansion coefficient. In the following, we present a detailed discussion of the evolution of the distinct anomalies with increasing Th content x.

3.1. The anomalies in the superconducting state at T_L ($x < x_{c1}$)

As described above, the anomaly at T_L is established by comparing thermal expansion with specific heat data. In Fig. 6 we plot the $\alpha(T)$ and $C(T)$ data sets for a UBe_{13} single crystal and for several doped $U_{1-x}Th_xBe_{13}$

polycrystals with $0.017 \leq x \leq 0.03$ using a common temperature scale. The same procedure to extract the "$T_{\rm L}$ anomaly" as described in the previous section is applied to the results of the doped sample $U_{0.983}Th_{0.017}Be_{13}$. Upon increasing x towards $x_{\rm c1}$, this low-T feature becomes progressively more pronounced and shifts to lower temperatures.

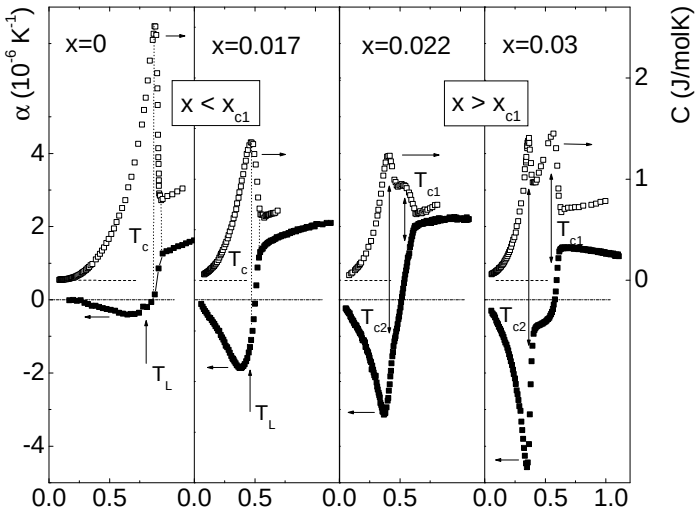

Fig. 6. Low-temperature specific heat (open symbols, right scale) and thermal expansion (closed symbols, left scale) on single-crystalline UBe_{13} and polycrystalline $U_{1-x}Th_xBe_{13}$ with $x = 0.017, 0.022$ and 0.03. The specific heat data for $x = 0.017$ and 0.022 are taken from Refs. [26] and [27], respectively, the thermal expansion and specific heat data of $x = 0.03$ from Ref. [14].

We have also measured the temperature dependence of the DC magnetization $M(T)$ for $U_{0.99}Th_{0.01}Be_{13}$ at a magnetic field of $B = \mu_0 H = 0.5\,\mathrm{T}$ [19]. In Fig. 7(a) we plot M/H *vs* T. Open and closed symbols denote zero-field (ZFC) and field-cooled (FC) data. The SC transition occurs at $T_{\rm c} = 0.63\,\mathrm{K}$, below which temperature a clear hysteresis begins. Whereas only a small additional feature is observed in the FC data, the ZFC data show a clear anomaly in the sc state, *i.e.* at 0.53 K. Its position, $T(B^*)$, almost coincides with $T_{\rm L}$ observed in $\alpha(T)$. In Fig. 7(b) we show the B–T phase diagram of $U_{0.99}Th_{0.01}Be_{13}$ determined by these magnetization measurements. The latter confirm the existence of a low-T anomaly at $T(B^*) = T_{\rm L}$ in $U_{0.99}Th_{0.01}Be_{13}$.

At $x = x_{\rm c1}$ $T_{\rm L}$ becomes close to $T_{\rm c}$. Beyond this concentration, the SC transition at $T_{\rm c1}(x)$ starts to separate again from a low-T anomaly at $T_{\rm c2}(x)$ which signals a true second-order phase transition. The transition

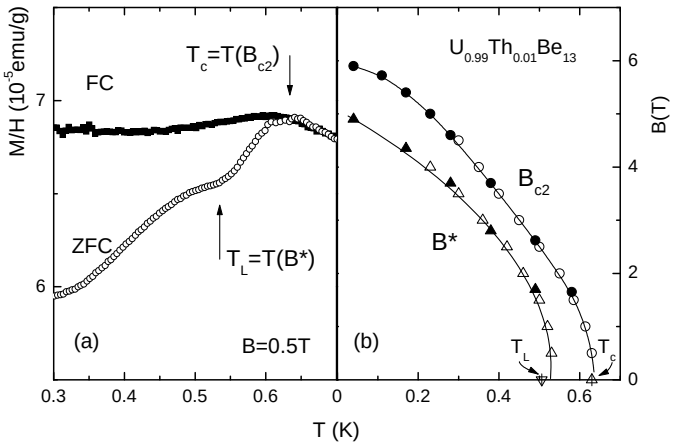

Fig. 7. (a) Field-cooled (FC) and zero-field-cooled (ZFC) magnetization of $U_{0.99}Th_{0.01}Be_{13}$ in an external field of 0.5 T as M/H *vs* T. (b) B–T diagram due to ZFC measurements including the SC phase transition at B_{c2} and the anomalies at B^*. Open symbols refer to temperature scans, closed symbols represent field scans. Data points for $B = 0$ are obtained by a thermal expansion measurement.

temperatures as derived from the usual equal-areas construction in α/T *vs* T are in good agreement with literature results [10, 27]. Comparison of the outward appearance of the "$T_{\rm L}$ anomaly" with the transition at $T_{\rm c2}$ strongly suggests that the phase-transition anomaly at $T_{\rm c2}$ for $x > x_{\rm c1}$ evolves out of the minimum structure at $T_{\rm L}$ in the subcritical concentration range. The shape as well as the sign of the anomaly at $T_{\rm L}$ in the thermal expansion are consistent with short-range AF correlations [14]. In this same reasoning the vertical phase boundary found near $x = x_{\rm c1}$ [20] might be ascribed to the formation of long-range AF order at $x > x_{\rm c1}$ and below $T = T_{\rm c2}$ [14].

Further arguments for the "$T_{\rm L}$ anomaly" being the precursor of the second phase transition at $T_{\rm c2}$ are provided by comparing the pressure dependences of $T_{\rm c}$, $T_{\rm c1}$, and $T_{\rm c2}$ and comparing the jump heights of the $\alpha(T)$ anomalies at $T_{\rm L}$ and $T_{\rm c}$ with those at $T_{\rm c2}$ and $T_{\rm c1}$, respectively. These values are shown as a function of x in Fig. 8. Fig. 8(a) displays the concentration dependence of $\partial T_{\rm c}/\partial p$ and $\partial T_{\rm c1}/\partial p$, deduced either from AC susceptibility measurements under hydrostatic pressure [15], open circles, or from the jump heights at $T_{\rm c}$ ($T_{\rm c1}$) in $\alpha(T)$ [28,29] and $C(T)$ [27] via the Ehrenfest relation, closed symbols. All pressure derivatives are negative. The absolute value of $\partial T_{\rm c}/\partial p$ increases only weakly at small Th concentration. Close to the first critical concentration $x_{\rm c1}$, however, this increase becomes quite large. Similar values are found for $\partial T_{\rm c1}/\partial p$ ($x \geq 0.03$) as for $\partial T_{\rm c}/\partial p$ ($x = 0$). The absolute value of the pressure dependence of $T_{\rm c2}$ is strongly enhanced prior to $x = x_{\rm c2}$ (closed triangles in Fig. 8).

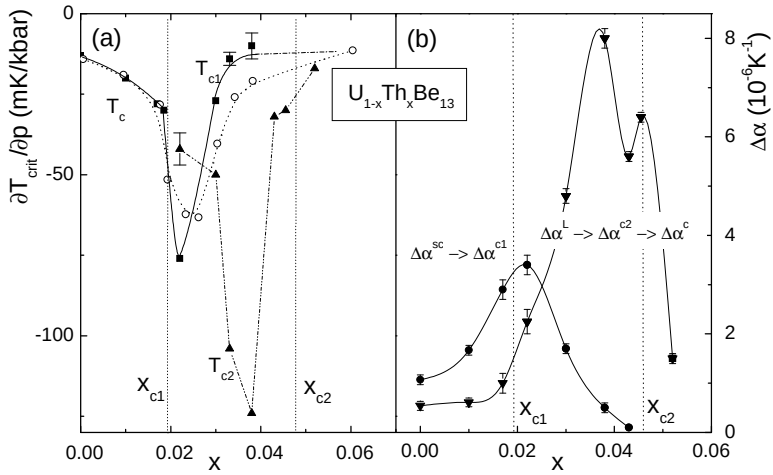

Fig. 8. (a) Pressure dependence of the critical temperature $T_{\rm crit}$ ($T_{\rm c}$, $T_{\rm c1}$, and $T_{\rm c2}$) $\partial T_{\rm crit}/\partial p$ *vs* x. Closed symbols correspond to pressure coefficients derived from the Ehrenfest relation. The value for $x = 0.0331$ is calculated by using $\Delta\alpha$ and ΔC values from Ref. [29]. Open circles mark the pressure coefficients of $T_{\rm c}$ and $T_{\rm c1}$ from susceptibility measurements under hydrostatic pressure [15]. (b) Magnitude of the absolute thermal expansion anomalies at $T_{\rm c}$ ($x < x_{\rm c1}$), $\Delta\alpha^{\rm sc}$, and $T_{\rm c1}$ ($x_{\rm c1} < x < x_{\rm c2}$), $\Delta\alpha^{\rm c1}$, as well as at $T_{\rm L}$ ($x < x_{\rm c1}$), $\Delta\alpha^{\rm L}$, $T_{\rm c2}$ ($x_{\rm c1} < x < x_{\rm c2}$), $\Delta\alpha^{\rm c2}$, and $T_{\rm c}$ ($x > x_{\rm c2}$), $\Delta\alpha^{\rm c}$, as a function of Th concentration.

The theoretical models mentioned before as well as a more recent one [30] predict different SC states below $T_{\rm c}$ ($x < x_{\rm c1}$) and $T_{\rm c1}$ [24, 25]. This prediction was based on seemingly different pressure derivatives of $T_{\rm c}$ ($x < x_{\rm c1}$) and $T_{\rm c1}$ [15]. However, $\partial T_{\rm c}/\partial p$ and $\partial T_{\rm c1}/\partial p$ behave uniformly with a maximum absolute value close to $x_{\rm c1}$, indicating some critical (pair-breaking) fluctuations, while $\partial T_{\rm c2}/\partial p$ behaves quite differently.

This is supported by the data shown in Fig. 8(b). Here, the evolution of the jump heights $|\Delta\alpha|$ at $T_{\rm c}$ and $T_{\rm c1}$ as a function of x are plotted for $x \leq 0.043$ (closed and open circles, respectively). As always, $\Delta\alpha^{\rm sc} = |\Delta\alpha(T_{\rm c})|$ and $\Delta\alpha^{\rm c1} = |\Delta\alpha(T_{\rm c1})|$ as well as $\Delta\alpha^{\rm c2} = |\Delta\alpha(T_{\rm c2})|$ are derived from equal-areas constructions in α/T *vs* T plots. The jump height of the anomaly $|\Delta\alpha^{\rm L}|$ at $T_{\rm L}$ is obtained in a similar way, *i.e.* by replacing its high-temperature flank by an idealized jump. The size and the sharpness of the minimum structure at $T_{\rm L}$ grow upon increasing x and pass continuously over into the sharper anomaly at $T_{\rm c2}$. $\Delta\alpha^{\rm sc}$ and $\Delta\alpha^{\rm c1}$ form a uniform curve with a maximum near $x = x_{\rm c1}$ as already found in the specific heat [27]. $\Delta\alpha^{\rm L}(x)$ is

also increasing as x approaches x_{c1}, but this increase becomes even stronger at higher concentration. $\Delta\alpha^{c2}(x)$ turns to $\Delta\alpha^{c}(x) = |\Delta\alpha(T_c)|$ for $x > x_{c2}$. The corresponding curve shows a global decline for $x > 0.038$ with a local minimum prior at $x = x_{c2}$, *i.e.* where $\Delta\alpha^{c1} \to 0$.

3.2. The anomalies at T_{max}

Another anomaly has been observed in resistivity, specific heat, and thermal expansion experiments performed on pure UBe_{13} [16,31,32]. In specific heat and thermal expansion measurements, the low-T N-state is dominated by a broad nearly field-independent maximum structure around 2 K. In thermal expansion measurements on $U_{1-x}Th_xBe_{13}$ with increasing x (≤ 0.03), this anomaly is found to shift to lower temperatures (*cf.* Fig. 9), and $T_{max}(x)$ is depressed in a linear function [32] (*cf.* Fig 5). $T_{max}(x)$ and $T_{c1}(x)$ were

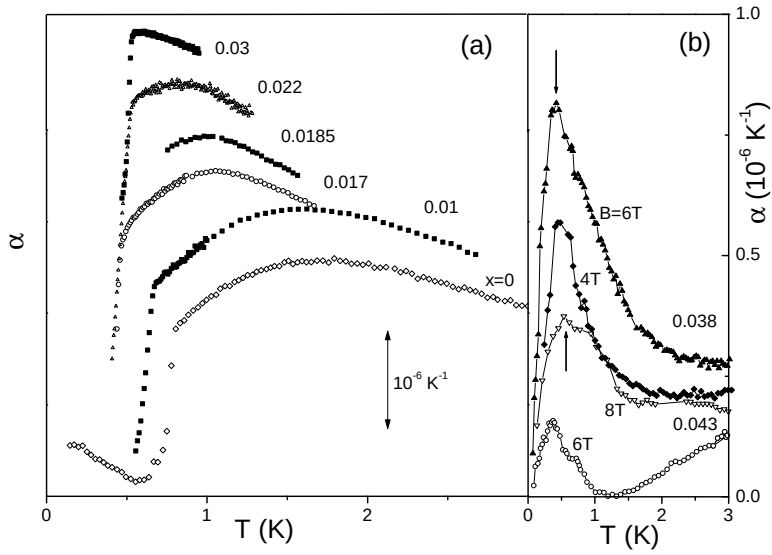

Fig. 9. (a) Low-temperature thermal expansion of single-crystalline UBe_{13} and polycrystalline $U_{1-x}Th_xBe_{13}$. A vertical shift of each data set has been employed for clarity. (b) By applying an overcritical field the maximum structure can be recovered for both $x = 0.038$ (closed symbols) and 0.043 (open symbols). Arrows mark the positions of the $\alpha(T, B)$ maxima.

found to intersect at $x = 0.03$, *i.e.* at the maximum of the T_{c1} *vs* x "dome". For $x \geq 0.038$, a negative contribution to the N-state thermal expansion, $\alpha_n(T)$, is found at low T. This feature can be easily suppressed by application of moderate magnetic fields for $x = 0.038$ and 0.043. At the same time a positive peak below $T = 1$ K is recovered whose position is slightly

shifted to higher T, if the field is increased (Fig. 9(b)). If we extrapolate this field-dependence to $B = 0$, we find the peak position to agree within experimental uncertainty with the continuation of the $T_{\max}(x)$ straight line established for $x \leq 0.03$ [19], *cf.* Fig 5.

Compared to the related maximum at $T \simeq 2\,\mathrm{K}$ in the T dependence of the electrical resistivity [16,33], the 2 K anomalies in $C(T)$ and $\alpha(T)$ of pure UBe_{13} show *(i)* a very weak magnetic field dependence, *(ii)* are less strongly shifted to lower T upon doping with Th, but *(iii)* exhibit a similar response to hydrostatic pressure, *i.e.* a shift to higher T. The microscopic origin of the anomalies at $T_{\max}$ is not resolved yet. Knetsch *et al.* [16], based upon their resistivity results, proposed itinerant magnetic fluctuations while Kromer *et al.* [28], due to the positive sign of the $\alpha(T)$ peak (Fig. 9), suggested more localized (Kondo-like) magnetic fluctuations. Alternatively, the anomaly might be ascribed to a non-magnetic, *e.g.* quadrupolar, origin due to its weak response to the application of a magnetic field.

3.3. The nature of the phase below T_{c2}

In Fig. 10 the thermal expansion and specific heat results are presented for $0.038 \leq x \leq 0.052$ displaying the evolution of the two phase transitions through the second critical point $x_{c2} \approx 0.0455$. In addition, results of AC-susceptibility measurements indicating the onset of superconductivity are also shown in Fig. 10. The jump at T_{c2} reaches a maximum value for $x = 0.038$ and decreases upon further increasing x. The discontinuity at the SC transition at T_{c1} in both thermodynamic quantities becomes strongly reduced when x exceeds 0.03, see also Fig. 8(b). For $x = 0.038$ ΔC^{c1} and $\Delta\alpha^{c1}$ are already strongly reduced [34]. For $x \geq 0.043$ they cannot be resolved anymore, though the $\chi_{AC}(T)$ data reveal the onset of superconductivity at $T_c^{\chi} > T_{c2}$. At $x > 0.0455$, T_c^{χ} is coinciding with T_{c2} as is illustrated in Fig. 10 for $x = 0.052$ and is labeled T_c in the following. Superconductivity is completely suppressed in $U_{0.93}Th_{0.07}Be_{13}$ [28].

The shape of the single phase-transition anomaly at T_c for $x > x_{c2}$ in both $\alpha(T)$ and $C(T)$ looks very similar to the anomaly at T_{c2} ($x_{c1} < x < x_{c2}$). Scaling the transition temperature and the jump height of the anomalies below and above x_{c2} to the position and absolute value of the negative peak, T_p and $\alpha_p|$, respectively, one finds that they all fall roughly on top of each other, see Fig. 11. This demonstrates clearly that the "T_{c2} anomaly" still exists beyond the second critical point [28]. Moreover, AC-susceptibility measurements show that the phase transition at T_c^{χ} is a SC one. For $x > 0.03$, the anomaly at T_{c1} is indicated only by a tiny anomaly which disappears as $x \to x_{c2}$. A SC transition at which no anomaly in either

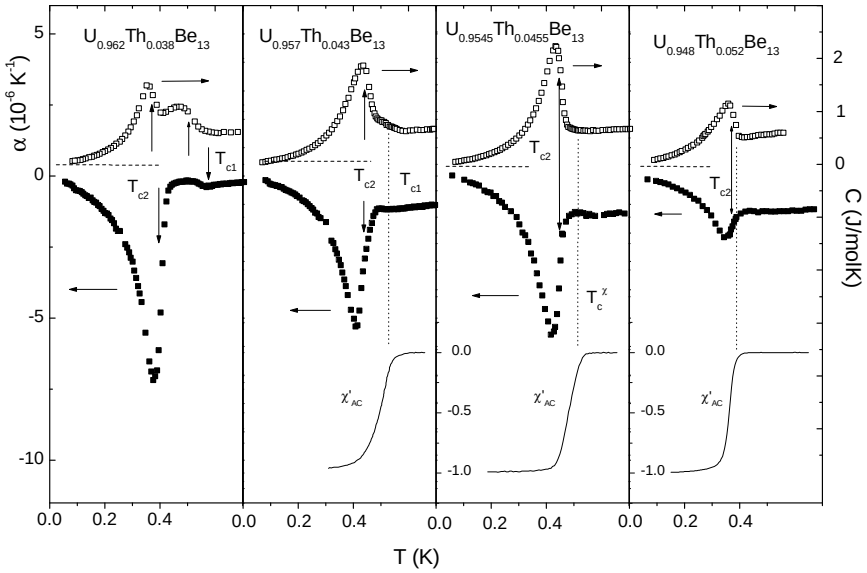

Fig. 10. Low-temperature specific heat (open symbols, right scale), thermal expansion (closed symbols, left scale), and AC susceptibility (solid line, inner scale) for polycrystalline $U_{1-x}Th_xBe_{13}$ with $0.038 \leq x \leq 0.052$. Vertical arrows mark the positions of phase transitions at T_{c1} and T_{c2}. Dotted vertical lines correspond to the SC nucleation temperatures deduced from AC susceptibility.

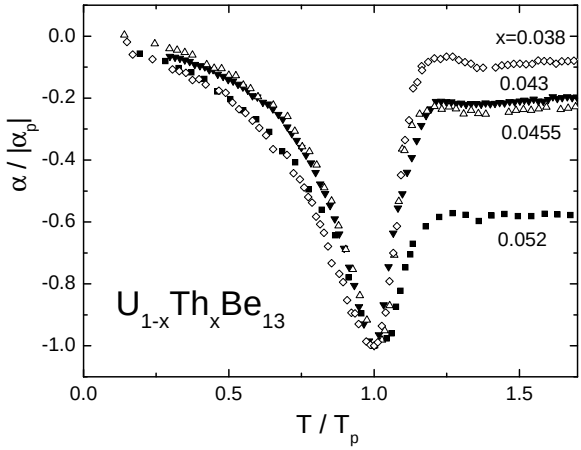

Fig. 11. Low-T thermal expansion coefficient scaled to the absolute maximum value of the "T_{c2} anomaly" ($x < 0.0455$) as well as of the "T_c anomaly" ($x \geq 0.0455$), $\alpha/|\alpha_p|$, *vs* temperature scaled to the respective temperature value, T/T_p, for $x =$ 0.038, 0.043, 0.0455 and 0.052.

the specific heat or the thermal expansion is observed points to gapless superconductivity due to strong pair breaking. It is straightforward to assume that the pair-breaking effect is caused by the fluctuations above $T_{\max}$.

As described above, these fluctuations leading to the maximum structure at $T_{\max}$ may be considered local Kondo fluctuations. They seem to freeze out gradually below $T_{\max}$. Thus, no significant influence on the SC state is expected for $x \leq 0.03$. For $x = 0.03$ where T_{c1} attains a local maximum the $T_{\max}(x)$ line intersects the $T_{c1}(x)$ line. The reduction of both T_{c1} as well as of the accompanying phase-transition anomalies in $C(T)$ and $\alpha(T)$ upon further increasing x, strongly suggest the onset of a very effective pair-breaking mechanism.

3.4. Normal state of $U_{1-x}Th_xBe_{13}$ ($x > x_{c2}$)

While the thermodynamic properties of the low-T N-state of $U_{1-x}Th_xBe_{13}$ with $x \leq 0.03$ are governed by a broad maximum structure, for $x > x_{c2}$, a negative thermal expansion peak shows up at low T (*cf.* Fig. 12(a)). The temperature at which the minimum occurs, $T_{\min}$, increases with increasing x. These values are included in the phase diagram of Fig. 5. By contrast, the absolute size of this minimum, $\alpha_{\min}$, decreases with increasing x, and relative weight is shifted to higher temperatures. In Fig. 12(b) the field dependence of $\alpha_n(T)$ is shown for $x = 0.07$. While $T_{\min}$ is almost field independent, the absolute value of $\alpha_n(T)$ is suppressed steadily. Even at $B = 8\,\mathrm{T}$, the highest field accessible, the expansion remains negative. As

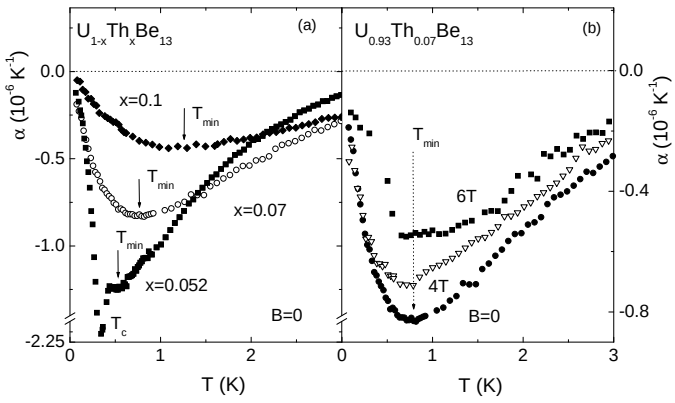

Fig. 12. (a) N-state thermal expansion behaviour $\alpha_n(T)$ for $U_{1-x}Th_xBe_{13}$ with $x > x_{c2}$. Arrows indicate the temperature, at which $\alpha_n(T)$ passes a minimum. (b) Magnetic field dependence of the thermal expansion coefficient of $U_{0.93}Th_{0.07}Be_{13}$. The minimum position at $T_{\min}$ is almost field independent.

reported in [19], in a plot $\alpha_n(T)/|\alpha_{\min}|$ *vs* $T/T_{\min}$ all curves fall on top of each other. $|\alpha_{\min}|$ is suppressed in a non-linear manner by magnetic fields. Low fields hardly affect $\alpha_n(T)$, whereas intermediate fields are efficient in strongly reducing $|\alpha_{\min}|$. For $x = 0.0455$ and 0.052 $\alpha_{\min}(B)$ saturates at high fields. In [19, 28], this negative $\alpha_n(T)$ anomaly has been related to inter-site correlations involving extremely small magnetic moments. In this scenario, the SC transition at T_c coincides with the "T_{c2} transition", *i.e.* a long-range AF one. The short-range AF correlations become, upon increasing the Th concentration, progressively frozen out at $T_{\min}$, *i.e.* well above the long-range ordering transition.

Assuming that for $x \simeq 0.1$, the $5f^2$ (U^{4+}) configuration with a low-lying non-magnetic Γ_3 CF-driven doublet state and the $5f^3$ (U^{3+}) configuration with a magnetic Γ_6 doublet ground state are almost degenerate, a negative $\alpha_n(T)$ anomaly may be explained alternatively, in the context of a two-channel Kondo model, by virtual f^2-f^3 fluctuations [35]. The field-induced suppression of the negative N-state contribution $\alpha_n(T)$ observed in $U_{1-x}Th_xBe_{13}$ with $x \geq 0.038$ may in this scenario be related to the Zeeman splitting of the magnetic $5f^3$ level which lifts the $5f^2/5f^3$ degeneracy. This may result in a suppression of the valence fluctuations due to the stabilization of the $5f^3$ ground-state configuration at the cost of the $5f^2$ valence state [19].

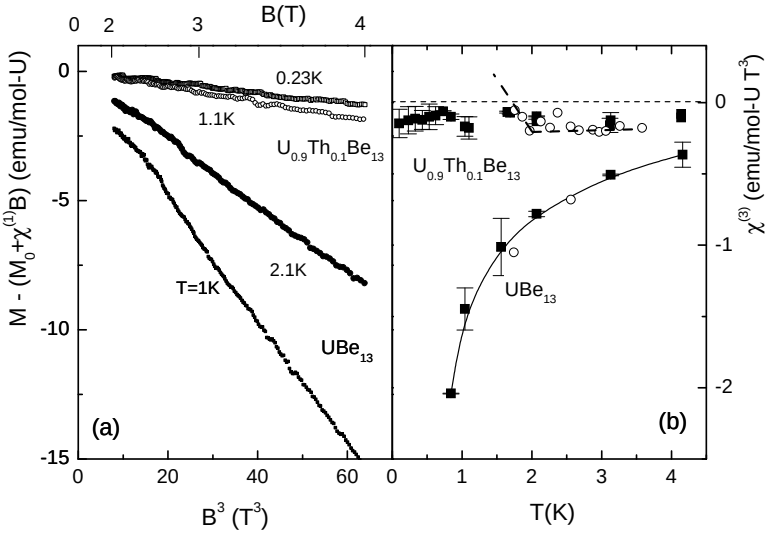

Fig. 13. (a) Non-linear susceptibility, $M - (M_0 + \chi^{(1)}\, B)$ *vs* B^3 of single-crystalline UBe_{13} and polycrystalline $U_{0.9}Th_{0.1}Be_{13}$. (b) Temperature dependence of $\chi^{(3)}$ for UBe_{13} and $U_{0.9}Th_{0.1}Be_{13}$. Open symbols and broken line refer to Ref. [36].

This latter scenario may also explain [19] the almost temperature-independent small (negative) non-linear susceptibility $\chi^{(3)}$ found for $U_{0.9}Th_{0.1}Be_{13}$ which strikingly contrasts with the apparent negative divergence of $\chi^{(3)}(T)$ in pure UBe_{13}, *cf.* Fig. 13. In fact, Schiller *et al.* [35] showed that, at least at higher T, a T-independent $\chi^{(3)}$ may originate in an intermediate-valence ground state of Uranium with 70% weight of the $5f^2$ configuration. On the other hand, a pure U-$5f^2$ configuration as proposed in [36] is unlikely since, owing to the $\chi^{(3)}(T)$ results of Fig. 13(b), the expected quadrupolar ordering occurs — if at all — at extremely low temperatures, $T < 50\,\mathrm{mK}$ [19].

4. Epilogue

We have discussed the low-T behaviour of the heavy-fermion metal UBe_{13} and of its thoriated variant $U_{1-x}Th_xBe_{13}$ ($x \leq 0.1$). In the pure compound, an unconventional (not yet fully identified) SC ground state competes with an also unconventional N-metallic state. The latter can be studied only in applied magnetic fields at lower temperatures, where it shows striking similarities to the N-state of other NFL superconductors, *e.g.* S-type $CeCu_2Si_2$ [37] and $CeNi_2Ge_2$ [38]. This hints at the vicinity of an AF QCP [39]. We propose that the low-lying 3D AF spin fluctuations responsible for the NFL properties of N-state UBe_{13} are those associated with the field-induced suppression of the "T_L anomaly", *i.e.* $T_L \to 0$ at $B \approx 4\,\mathrm{T}$ (*cf.* Fig. 3(b)).

The "T_L anomaly" in $\alpha(T)$ ($x < x_{c1}$) seems to indicate the freezing out of AF short-range correlations — due to its magnetic-field dependence and its negative sign. As is evident from Figs. 6 and 8b, this unique feature has to be considered the precursor of the lower of the two second-order phase transitions that occur at T_{c1} and T_{c2} for $x_{c1} < x < x_{c2}$. It is, therefore, tempting to assume that long-range AF order (with extremely low ordered moment [21]) forms below $T = T_{c2}$, in agreement with conclusions drawn from early ultrasound-attenuation measurements [22]. Further, as suggested in Fig. 6, the SC states below and above $x = x_{c1}$ are not necessarily different, and the strong T_c depression observed at this concentration may be due to some critical fluctuations near the long-range ordered (AF) phase transition which occurs at x_{c1} [20].

It was shown that, in addition to T_L, T_{c2} and T_c, T_{c1}, there exists a characteristic temperature, T_{max}, at which a pronounced positive $\alpha(T)$ maximum occurs. $T_{max} \simeq 2\,\mathrm{K}$ (in pure UBe_{13}) is depressed in a linear function upon doping with Th (Fig. 5). Though its origin is presently unclear, this unique feature has two important consequences: *(i)* As $T_{max} \to 0$ near $x = x_{c2}$, the SC transition at T_{c1}, and the transition at T_{c2} merge. For $x > x_2$, only one (SC) transition can be resolved, whose outward appearance (according

to our thermal expansion experiments) is very similar to that of the "T_{c2} transition" in the critical concentration range, *cf.* Fig 11. *(ii)* $T_{max}(x)$ intersects the $T_{c1}(x)$ "dome" at its local maximum ($x \simeq 0.03$). When increasing the Th concentration further ($T_{max} < T_{c1}$), the thermodynamic (α, C) signatures of the SC transition at T_{c1} become less pronounced and disappear completely as $x \to x_{c2}$ (Fig. 10). This implies either a vanishing of the T_{c1} transition as a whole or a vanishing of the SC gap in the presence of a finite SC order parameter ("gapless superconductivity"). In the first case (T_{c1} transition vanishes), the "T_{c2} anomaly" would presumably have a SC component not only for $x > x_{c2}$, but already in the critical concentration range $x_{c1} < x < x_{c2}$. In the second case (transition into a gapless SC state at T_{c1} persists), the "T_{c2} transition" is pinned to the SC one at $T = T_c$ for $x > x_{c2}$. T_c is gradually depressed and vanishes near $x_c \simeq 0.07$. However, a broad negative $\alpha_n(T)$ that develops at $T_{min} > T_c$ and appears to be intimately related to the "T_{c2} transition" is stabilized upon increasing x. T_{min} increases by more than a factor of two when going to $x = 0.1$. Though $T_{min}(x)$ seems to be the continuation of the $T_L(x)$ and $T_{c2}(x)$ line in the phase diagram of Fig. 5 and despite its negative sign, this $\alpha_n(T)$ anomaly shows a magnetic field dependence that differs from that of $T_L(x)$, $T_{c2}(x)$: while the latter are depressed by the field, T_{min} is almost field-independent.

Finally, in an intermediate-valence scenario, the U-$5f^3$ configuration is presumably the dominating one for $x = 0$, while the U-$5f^2$ configuration seems to dominate for $x = 0.1$. Such an assignment is suggested by the very different temperature dependences of the non-linear susceptibilities of UBe_{13} and $U_{0.9}Th_{0.1}Be_{13}$ (Fig. 13). This appears somewhat counter-intuitive in view of the volume expansion caused by the doping with Th, which would favor the $5f^3$ state. We suspect, therefore, that this valence change is governed by the change in the chemical potential when substituting Th^{4+} for U^{3+} ions.

In conclusion, it is fair to state that the low-T properties of the NFL superconductor UBe_{13} as well as the rich T–x phase diagram of $U_{1-x}Th_xBe_{13}$ pose a number of new challenges for and will, therefore, remain on the agenda of future research.

One of us (FS) gratefully acknowledges a fruitful conversation with Frithjof B. Anders. Work at Dresden was carried out within the ESF project "FERLIN" while work at Florida was supported by the US Department of Energy, contract No. De-FG05-86ER45268.

REFERENCES

[1] For a review, see, *e.g.* N. Grewe, F. Steglich, *Handbook on the Physics and Chemistry of Rare Earth*, Vol. 14 eds K.A. Gschneidner, L. Elsevier, Amsterdam 1991, p. 343.

[2] G.R. Stewart, *Rev. Mod. Phys.* **73**, 797 (2001).

[3] F. Steglich, J. Aarts, C.D. Bredl, W. Lieke, D. Meschede, W. Franz, H. Schäfer, *Phys. Rev. Lett.* **43**, 1892 (1979).

[4] C. Petrovic, P.G. Pagliuso, M.F. Hundley, R. Movshovich, J.L. Sarrao, J.D. Thompson, Z. Fisk, P. Monthoux, *J. Phys.: Condens. Matt.* **13**, L337 (2001).

[5] H.R. Ott, H. Rudigier, Z. Fisk, J.L. Smith, *Phys. Rev. Lett.* **50**, 1595 (1983).

[6] D.L. Cox, *Phys. Rev. Lett.* **59**, 1240 (1987).

[7] R. Felten, F. Steglich, G. Weber, H. Rietschel, F. Gompf, B. Renker, J. Beuers, *Europhys. Lett.* **2**, 323 (1986).

[8] S.L. Cooper, M.V. Klein, Z. Fisk, J.L. Smith, H.R. Ott, *Phys. Rev.* **B35**, 2615 (1987).

[9] A.P. Ramirez, P. Chandra, P. Coleman, Z. Fisk, J.L. Smith, H.R. Ott, *Phys. Rev. Lett.* **73**, 3018 (1994).

[10] H.R. Ott, H. Rudigier, Z. Fisk, J.L. Smith, *Phys. Rev.* **B31**, 1651 (1985).

[11] C. Langhammer, R. Helfrich, A. Bach, F. Kromer, M. Lang, T. Michels, M. Deppe, F. Steglich, G.R. Stewart, *J. Magn. Magn. Mater.* **177-181**, 443 (1998).

[12] H.R. Ott, H. Rudigier, T.M. Rice, K. Ueda, Z. Fisk, J.L. Smith, *Phys. Rev. Lett.* **52**, 1915 (1984).

[13] R. Helfrich, Dissertation, TU Darmstadt (1997), unpublished.

[14] F. Kromer, R. Helfrich, M. Lang, F. Steglich, C. Langhammer, A. Bach, T. Michels, J.S. Kim, G.R. Stewart, *Phys. Rev. Lett.* **20**, 4476 (1998).

[15] S.E. Lambert, Y. Dalichaouch, M.B. Maple, *Phys. Rev. Lett.* **13**, 1619 (1986).

[16] E.A. Knetsch, Dissertation, University of Leiden (1993), unpublished; E.A. Knetsch, G.J. Nieuwenhuys, J.A. Mydosh, R.H. Heffner, J.L. Smith, *Physica B* **186-188**, 251 (1993).

[17] P. Gegenwart, Dissertation, TU Darmstadt (1997), unpublished; F. Steglich, P. Gegenwart, R. Helfrich, C. Langhammer, P. Hellmann, L. Donnevert, C. Geibel, M. Lang, G. Sparn, W. Assmus, G.R. Stewart, A. Ochiai, *Z. Phys.* **B103**, 235 (1997).

[18] T. Moriya, T. Takimoto, *J. Phys. Soc. Jpn.* **64**, 960 (1995).

[19] F. Kromer, N. Oeschler, T. Tayama, K. Tenya, T. Cichorek, M. Lang, F. Steglich, J. S. Kim, G. R. Stewart, *J. Low Temp. Phys.* **126**, 815 (2002).

[20] R.J. Zieve, D.S. Jin, T.F. Rosenbaum, J.S. Kim, G.R. Stewart, *Phys. Rev. Lett.* **72**, 756 (1994).

[21] R.H. Heffner, J.L. Smith, J.O. Willis, P. Birrer, C. Baines, F.N. Gygax, B. Hitti, E. Lippelt, H.R. Ott, A. Schenk, E.A. Knetsch, J.A. Mydosh, D.E. MacLaughlin, *Phys. Rev. Lett.* **65**, 2816 (1990).

[22] B. Batlogg, D. Bishop, B. Golding, C.M. Varma, Z. Fisk, J.L. Smith, H.R. Ott, *Phys. Rev. Lett.* **12**, 1319 (1985).

[23] U. Rauchschwalbe, F. Steglich, G.R. Stewart, A.L. Giorgi, P. Fulde, K. Maki, *Europhys. Lett.* **3**, 751 (1987).

[24] P. Kumar, P. Wölfle, *Phys. Rev. Lett.* **17**, 1954 (1987).

[25] M. Sigrist, T.M. Rice, *Phys. Rev.* **B39**, 2200 (1989).

[26] D.S. Jin, T.F. Rosenbaum, J.S. Kim, G.R. Stewart, *Phys. Rev.* **B49**, 1540 (1994).

[27] E.-W. Scheidt, T. Schreiner, P. Kumar, G.R. Stewart, *Phys. Rev.* **B58**, 15153 (1998).

[28] F. Kromer, M. Lang, N. Oeschler, P. Hinze, C. Langhammer, F. Steglich, *Phys. Rev.* **B62**, 12477 (2000).

[29] H.R. Ott, H. Rudigier, E. Felder, Z. Fisk, J.L. Smith, *Phys. Rev.* **B33**, 126 (1986).

[30] V. Martisovits, G. Zaránd, D.L. Cox, *Phys. Rev. Lett.* **84**, 5872 (2000).

[31] H.M. Mayer, U. Rauchschwalbe, C.D. Bredl, F. Steglich, H. Rietschel, H. Schmidt, H. Wühl, J. Beuers, *Phys. Rev.* **B33**, 3168 (1986).

[32] M. Lang, R. Helfrich, F. Kromer, C. Langhammer, F. Steglich, G.R. Stewart, J.S. Kim, *Physica B* **259-261**, 608 (1999).

[33] U. Rauchschwalbe, F. Steglich, H. Rietschel, *Europhys. Lett.* **1**, 71 (1986).

[34] Note that discrepancies in the phase-transition temperatures between specific heat and thermal expansion results for $U_{0.962}Th_{0.038}Be_{13}$ may indicate small differences in the actual Th concentration for the two samples studied.

[35] A. Schiller, F.B. Anders, D.L. Cox, *Phys. Rev. Lett.* **81**, 3235 (1998).

[36] F.G. Aliev, H. El Mfarrej, S. Vieira, R. Villar, J.L. Martinez, *J. Phys.: Condens. Matter* **8**, 9807 (1995).

[37] P. Gegenwart, C. Langhammer, C. Geibel, R. Helfrich, M. Lang, G. Sparn, F. Steglich, R. Horn, L. Donnevert, A. Link, W. Assmus, *Phys. Rev. Lett.* **81**, 1501 (1998).

[38] P. Gegenwart, F. Kromer, M. Lang, G. Sparn, C. Geibel, F. Steglich, *Phys. Rev. Lett.* **82**, 1293 (1999).

[39] We note that the NFL phenomenology established for UBe_{13} is at striking variance to the one expected for the quadrupolar Kondo effect [6].